Supporting information

Development of a stable peptide-based PET tracer for detecting CD133-expressing cancer cells

Kuan Hu[1,#], Xiaohui Ma[3,#], Lin Xie[1], Yiding Zhang[1], Masayuki Hanyu[1], Honoka Obata[1], Lulu Zhang[1], Kotaro Nagatsu[1], Hisashi Suzuki[1], Rui Shi[4,*], Weizhi Wang[2,*], Ming-Rong Zhang[1,*]

[1]Department of Advanced Nuclear Medicine Sciences, National Institute of Radiological Sciences, National Institutes for Quantum and Radiological Science and Technology, Chiba, 263-8555, Japan.

[2]School of Chemistry and Chemical Engineering, Beijing Institute of Technology, Beijing 100081, P. R. China.

[3]Department of Vascular Surgery, General Hospital of People's Liberation Army, Beijing 100853, P. R. China

[4]Institute of Traumatology and Orthopaedics Beijing Jishuitan Hospital Beijing Laboratory of Biomedical Materials Beijing 100035, P. R. China

Contents

1. Solid-phase peptide synthesis of radiotracer precursors

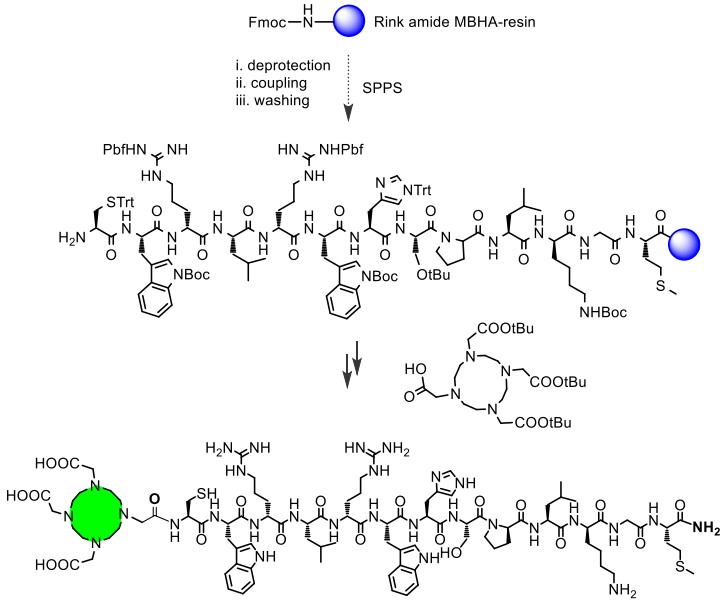

Scheme S1. Fmoc-based solid-phase peptide synthesis of CM-1.

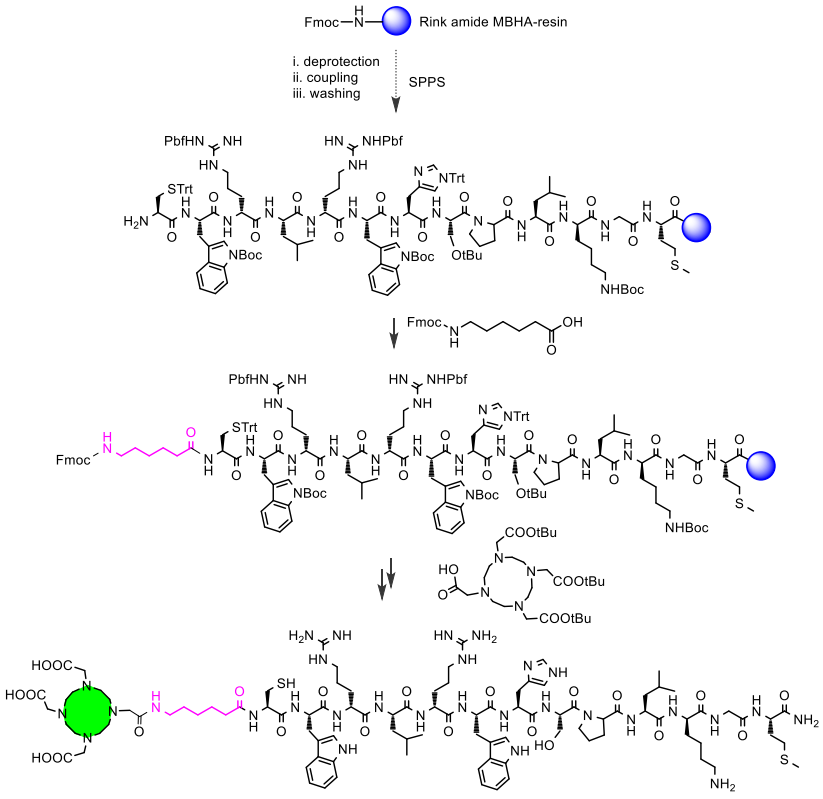

Scheme S2. Fmoc-based solid-phase peptide synthesis of CM-2.

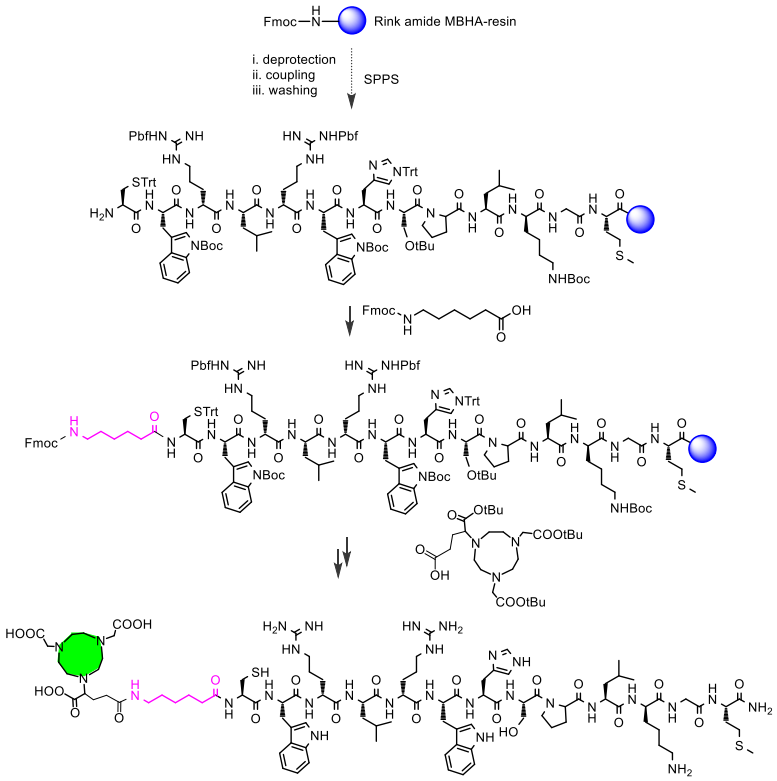

Scheme S3. Fmoc-based solid-phase peptide synthesis of CM-3.

2. PET quantification of region of interest and ex vivo biodistribution data

Table S1. Quantification of radioactivity in the Huh-7 tumors, liver, and kidney from BALB/C nude mice at different time points (57.5 min, 3.5 h, 18 h, 25 h, and 38 h) after i.v. injection of [^{64}Cu]CM-2 based on the PET-CT images. The radioactivity in organs was expressed as %injection dose per gram body weight (%ID/g). Data represent the mean ± SD, n = 4.

	PET quantification (%ID/g)					
Time	**57.5 min**	**4 h**	**9 h**	**18 h**	**30 h**	**55 h**
Tumor	1.70 ± 0.07	2.19 ± 0.20	2.78 ± 0.22	3.45 ± 0.41	3.80 ± 0.29	4.05 ± 0.37
Liver	8.02 ± 0.62	7.91 ± 0.90	8.01 ± 0.62	6.78 ± 0.45	6.18 ± 0.24	5.05 ± 0.19
Kidney	13.80 ± 0.80	11.04 ± 1.31	9.35 ± 0.97	5.34 ± 0.40	4.14 ± 0.78	2.74 ± 0.20

Table S2. Biodistribution of [^{64}Cu]CM-2 at 1, 2, 6, and 18 hours after i.v. injection (n = 3 per time point) in Huh-7 tumor-bearing BALB/C nude mice. T/B means tumor-to-blood ratio and T/M means tumor-to-muscle ratio. Data represent the mean ± SD, n = 3.

	[^{64}Cu]CM-2			
	1 h	2 h	6 h	18 h
Blood	1.91 ± 0.04	1.47 ± 0.16	1.28 ± 0.13	0.93 ± 0.14
Heart	2.08 ± 0.15	2.33 ± 0.42	2.79 ± 0.16	2.13 ± 0.36
Lung	3.70 ± 0.27	4.14 ± 0.63	4.88 ± 0.37	4.39 ± 0.47
Liver	17.35 ± 2.33	17.24 ± 0.97	15.05 ± 1.34	10.55 ± 0.82
Pancreas	1.37 ± 0.19	1.27 ± 0.27	1.56 ± 0.15	1.19 ± 0.09
Spleen	2.03 ± 0.09	2.08 ± 0.24	2.71 ± 0.27	2.78 ± 0.28
Kidney	50.14 ± 7.26	44.66 ± 1.35	27.72 ± 2.54	12.12 ± 0.80
Stomach	2.93 ± 0.64	2.25 ± 0.55	3.27 ± 1.33	2.34 ± 0.18
S. intestine	5.79 ± 1.42	5.12 ± 1.32	3.78 ± 0.57	3.52 ± 0.43
Int. lym. node	2.58 ± 0.43	2.02 ± 1.31	2.43 ± 0.24	1.54 ± 0.12
Muscle	0.58 ± 0.05	0.50 ± 0.09	0.45 ± 0.01	0.55 ± 0.32
Bone	1.17 ± 0.21	1.20 ± 0.21	1.23 ± 0.02	0.81 ± 0.35
Ovaries	1.58 ± 0.02	1.23 ± 0.72	2.10 ± 0.12	1.08 ± 0.17
Bladder	2.10 ± 0.50	1.54 ± 0.09	1.34 ± 0.21	1.25 ± 0.19
Huh7	3.77 ± 0.43	4.23 ± 0.62	6.89 ± 1.08	6.19 ± 0.69
Brain	0.15 ± 0.01	0.17 ± 0.02	0.21 ± 0.02	0.24 ± 0.02
T/B	1.97	2.87	5.39	6.67
T/M	6.45	8.42	15.19	11.18

Table S3. Quantification of radioactivity in the B16F10 tumors, liver, and kidney from B16F10 tumor-baring C57BL/6J mice at different time points (57.5 min, 3.5 h, 18 h, 25 h, and 38 h) after i.v. injection of [^{64}Cu]CM-2 based on the PET-CT images. The radioactivity in organs was expressed as %injection dose per gram body weight (%ID/g). Data represent mean ± SD, n = 4.

PET quantification (%ID/g)					
Time	**57.5 min**	**3.5 h**	**18 h**	**25 h**	**38 h**
Tumor	1.69 ± 0.13	1.95 ± 0.17	1.93 ± 0.10	1.93 ± 0.15	1.75 ± 0.06
Liver	9.41 ± 1.40	10.53 ± 0.28	6.23 ± 0.41	6.78 ± 0.36	4.48 ± 0.29
Kidney	15.07 ± 1.59	12.13 ± 0.97	4.45 ± 0.58	3.75 ± 0.34	2.80 ± 0.29

Table S4. Biodistribution of [^{64}Cu]CM-2 at 0.5, 2, 18, and 30 hours after i.v. injection (n = 3 per time point) in B16F10 tumor-bearing C57BL/6J mice. T/B means tumor-to-blood ratio and T/M means tumor-to-muscle ratio. Data represent the mean ± SD, n = 3.

	[^{64}Cu]CM-2			
	0.5 h	2 h	18 h	30 h
Blood	3.15 ± 0.14	1.68 ± 0.13	0.86 ± 0.08	0.96 ± 0.01
Heart	2.20 ± 0.25	2.09 ± 0.07	1.91 ± 0.24	2.34 ± 0.14
Lung	6.05 ± 0.08	7.29 ± 0.20	5.14 ± 0.52	4.92 ± 0.35
Thymus	2.46 ± 0.77	2.18 ± 0.18	1.31 ± 0.32	1.32 ± 0.03
Liver	23.92 ± 4.42	20.72 ± 0.77	11.12 ± 1.61	16.03 ± 1.18
Pancreas	1.60 ± 0.14	1.47 ± 0.10	1.03 ± 0.12	1.18 ± 0.06
Spleen	2.39 ± 0.49	1.98 ± 0.07	1.33 ± 0.10	1.84 ± 0.39
Kidney	53.20 ± 7.97	39.88 ± 2.10	7.58 ± 0.48	7.45 ± 0.77
Stomach	6.82 ± 0.93	6.38 ± 2.33	1.20 ± 0.20	1.66 ± 0.12
S. intestine	12.98 ± 3.76	9.76 ± 1.03	3.29 ± 0.35	2.71 ± 0.11
Intest. lym.node	6.17 ± 2.46	1.64 ± 0.23	0.99 ± 0.24	0.87 ± 0.05
Muscle	0.78 ± 0.10	0.46 ± 0.03	0.32 ± 0.02	0.43 ± 0.03
Bone	2.06 ± 0.19	1.83 ± 0.08	1.29 ± 0.16	1.21 ± 0.09
Testis	1.33 ± 0.40	0.86 ± 0.05	0.70 ± 0.08	0.80 ± 0.04
B16F10	4.67 ± 0.80	4.99 ± 0.46	3.17 ± 0.27	2.98 ± 0.31
Brain	0.22 ± 0.02	0.23 ± 0.01	0.25 ± 0.03	0.29 ± 0.02
T/B	1.48	2.98	3.70	3.10
T/M	5.96	10.76	9.94	7.02

3. Summary of the characteristics of the reported CD133 radiotracers

Table S5. Overview of the CD133 radiotracers in references.

Entry	*Tracer name*	*Molecular type*	*Imaging mode*	*Tumor model*	*Features*	*Reference*
1	^{64}Cu-NOTA-AC133	mAb	PET	U251 and NCH421k gliomas	High quality image with outstanding tumor-to-background contrast; best imaging window: 24-48 hours after injection	1
2	^{131}I-AC133	mAb	SPECT	LoVo tumors	High blood retention, low resolution; best imaging window: 5-7 days after injection	2
3	[^{89}Zr]Zr-HA10	IgG	PET	CWR-R1^{CD133} prostate cancer	High radiochemical purity; best imaging window: 24-72 hours after injection; specific for late-stage AVPC	3
4	[^{131}I]CD133	mAb	SPECT	HT29 colon cancer cell	Low sensitivity; best imaging window: 5-7 days after injection	4
5	[^{89}Zr]Zr-DFO-RW03	antibody	PET	HT29 colon cancer cell	High specific activity and affinity; High liver uptake; best imaging window: 96 hours after injection	5
6	^{68}Ga-DOTA-LS7	peptide	PET	HCT116 and Lovo cell-derived tumors	Small molecular size, low liver uptake; fast imaging with the best imaging time: 90 min post-injection	6
7	^{64}Cu-CM-2	peptide	PET	Huh-7, B16F10, U87MG, and Bowes	High stability, high tumor-to-background contrast, fast renal excretion; flexible imaging window; high liver retention	Current study

4. Summary of the peptide precursors

Table S6. Calculated and Founded m/z are presented as $[M+1H]^+/[M/2+H]^+/[M/3+H]^+$

Name	**Sequence**	**Formula**	**Calculated mass**	**Found mass**
CM-1	DOTA-CWRLRWHSPLKGM-OH	$C_{92}H_{142}N_{28}O_{22}S_2$	2055.03	686.5
CM-2	DOTA-Ahx-CWRLRWHSPLKGM-OH	$C_{98}H_{153}N_{29}O_{23}S_2$	2169.12	1085.6
CM-3	NODAGA-Ahx-CWRLRWHSPLKGM-OH	$C_{97}H_{150}N_{28}O_{23}S_2$	2140.09	714.71

5. Supplementary figures

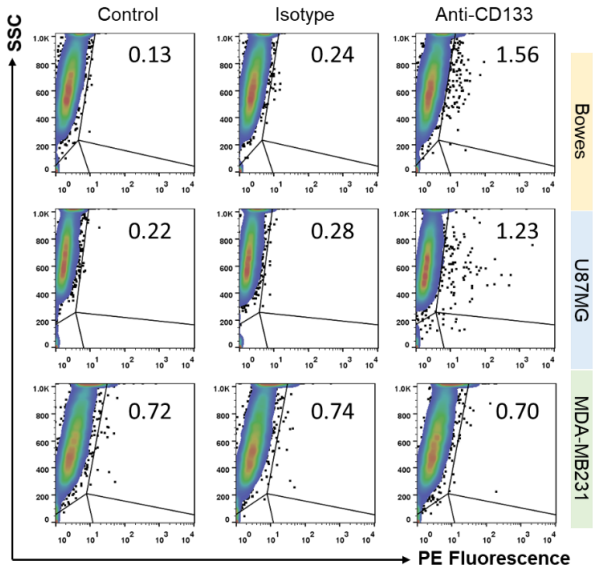

Figure S1. Flow cytometry analysis of the expression level of CD133 protein in Bowes, U87MG, and MDA-MB23 cell lines.

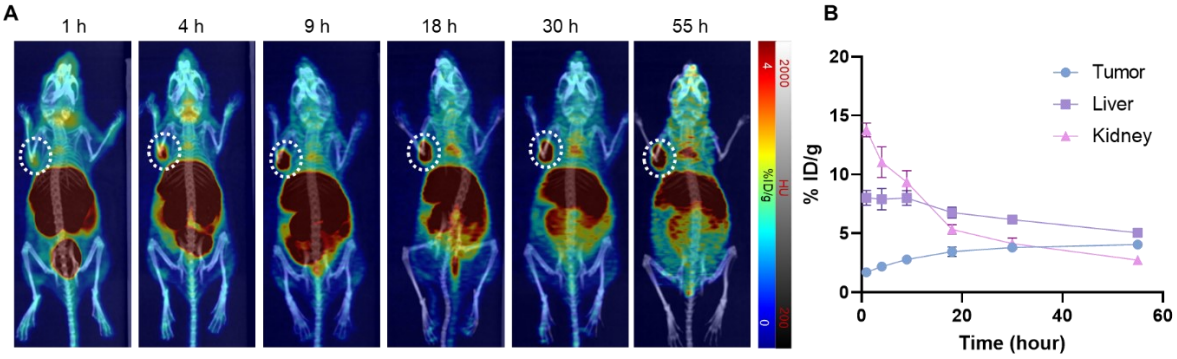

Figure S2. (A) Series of co-registered PET-CT maximum intensity projections (MIPs) at different time points postinjection from Huh7-bearing BALB/C nude mice. The white dashed circles indicate the Huh7 tumors. Animals were injected with approximately 17 MBq (0.2 mL, approximately 0.5 nmol of CM-2) of the tracers per mouse via the tail vein. (B) Time-activity curves of the tumor, liver, and kidney. The values were quantified based the PET images. Data represent the mean ± SD, *n* =3.

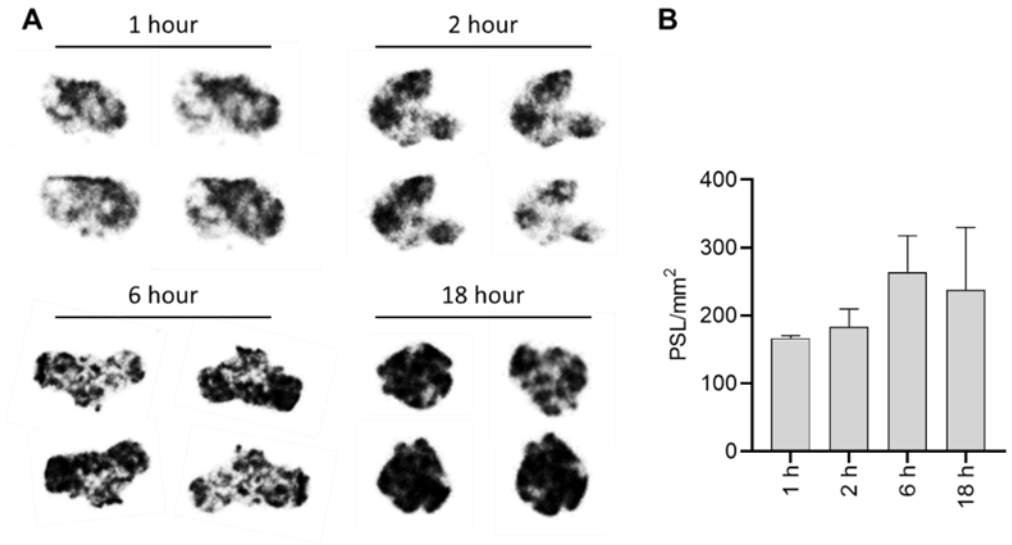

Figure S3. (A) *Ex vivo* autoradiography shows the accumulative uptake and distribution of [^{64}Cu]CM-2 in Huh-7 tumors at different time points after injection. Representative tumor sections at different time points are from different mice. (B) Quantitative analysis for uptake (PSL/mm^2; mean ± SD, >4 tissue sections for each time points.

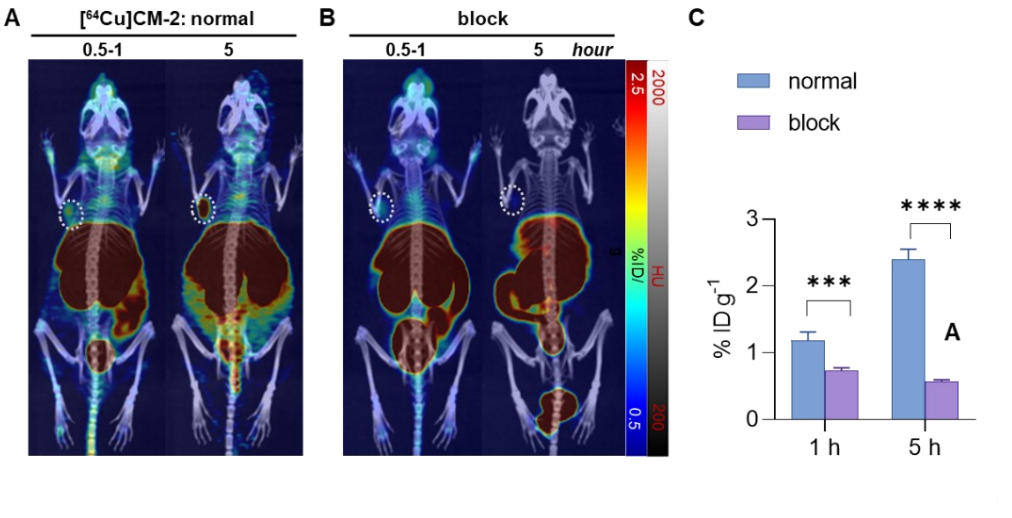

Figure S4. (A) Representative co-registered PET-CT MIP images from Huh-7 mice administrated with [^{64}Cu]CM-2 (17 MBq, 0.2 mL, approximately 0.5 nmol of CM-2). (B) Representative co-registered MIPS images from Huh-7 mice co-administered with [^{64}Cu]CM-2 (17 MBq, approximately 0.5 nmol of CM-2) and an excess of CM-2 (0.2 mg per mouse). The white dashed circles indicate the B16F10 tumors. (C) Quantitative analysis of tracer uptake in Huh-7 tumors from normal and block mice. Comparisons were performed using unpaired two-tailed Student's t-test. Data are presented as the mean ± SD, $n = 3$, ***$P < 0.001$, ****$P < 0.0001$.

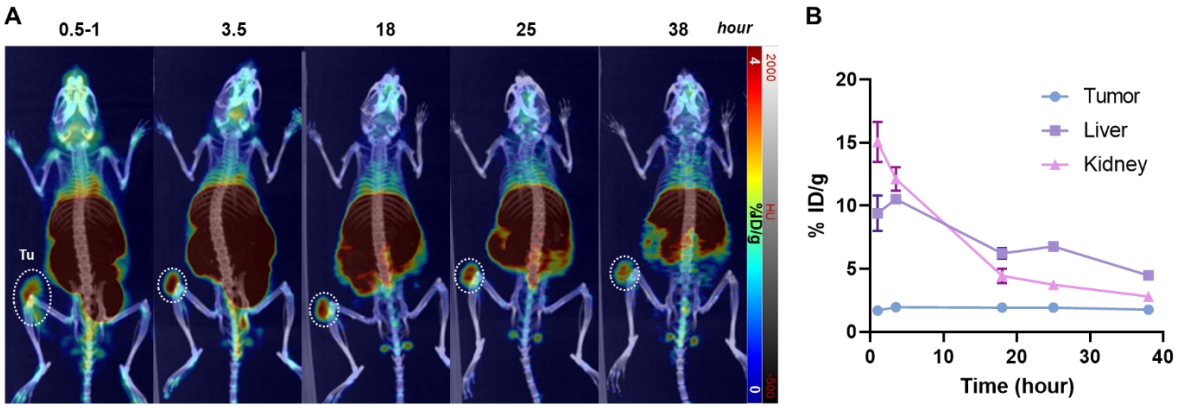

Figure S5. (A) Series of co-registered PET-CT MIPs at different time points postinjection from B16F10-bearing C57BL/6J mice. The white dashed circles indicate the B16F10 tumors. Animals were injected with approximately 17 MBq (0.2 mL, approximately 0.5 nmol of CM-2) of the tracers per mouse via the tail vein. (B) Time-activity curves of the tumor, liver, and kidney. The values were quantified based the PET images. Data represent the mean ± SD, *n* =3.

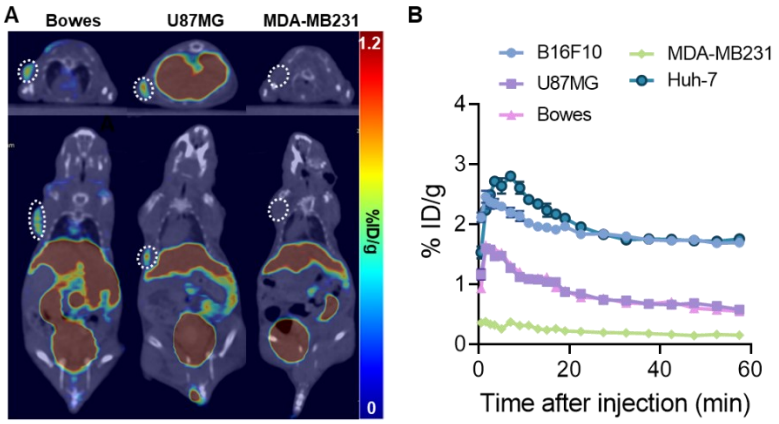

Figure S6. (A) Co-registered sectional PET-CT images of mice bearing Huh-7, Bowes, U87MG, or MDA-MB231 xenograft tumors at 35-55 min after i.v. injection of [^{64}Cu]CM-2 (17 MBq/mouse, 0.2 mL, approximately 0.5 nmol of CM-2). Upper panels: axial view; down panels: coronal view. White dashed circles indicate the xenograft tumors. (B) PET image-derived region-of-interest (ROI) curves of different tumors from 0 to 55 min after i.v. injection of [^{64}Cu]CM-2. (C) AUC derived from the corresponding ROI curves of tumors in panel B. Statistics analysis was performed using two-way ANOVA analysis, followed by Bonferroni's multiple comparisons test, $n = 4$, ***$P < 0.001$.

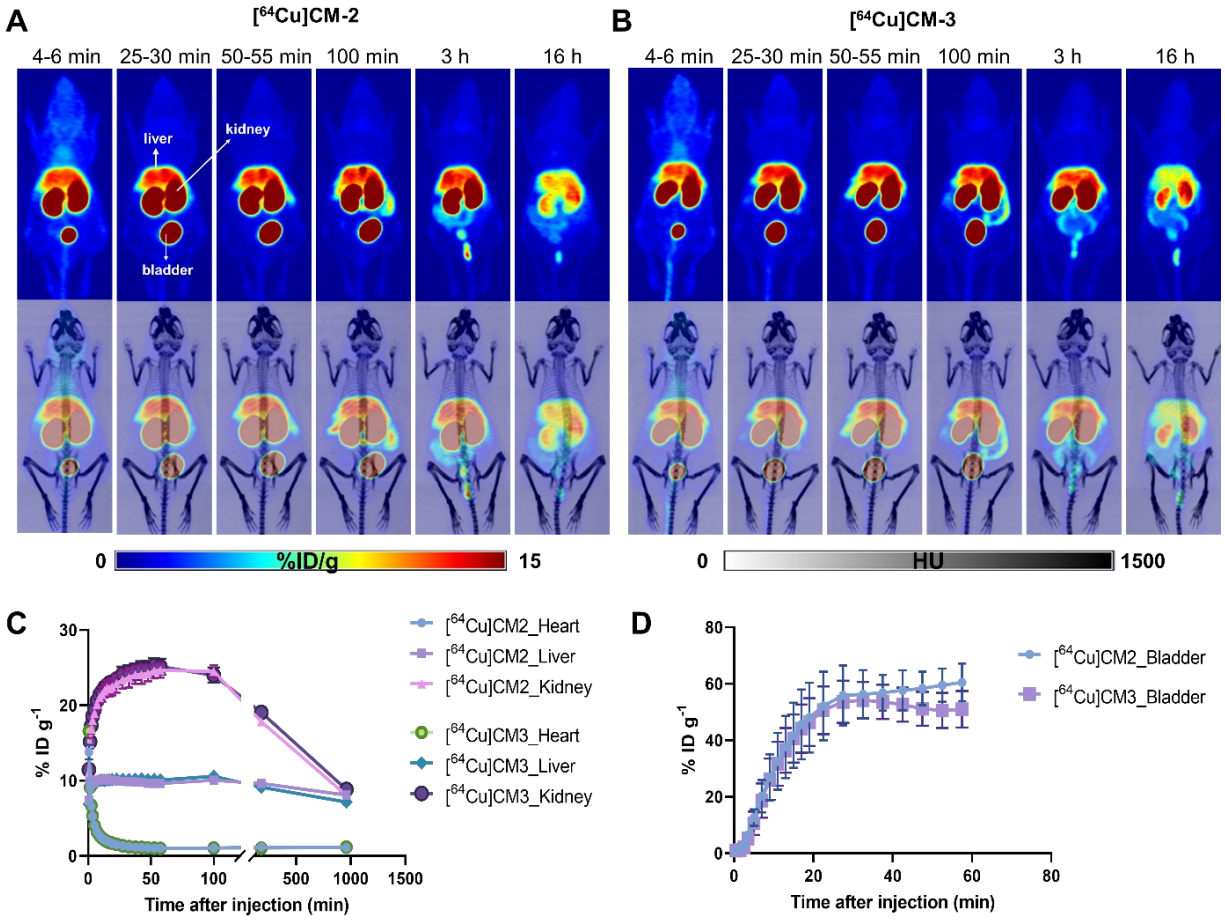

Figure S7. Series of MIPs (top panel) and co-registered PET-CT MIPs (bottom panel) at different time points from normal BALB/C nude mice after intravenous injection of (A) [^{64}Cu]CM-2 and (B) [^{64}Cu]CM-3. Animals were injected with approximately 17 MBq (0.2 mL, approximately 0.5 nmol of CM-2) of the tracers per mouse via the tail vein. (C) Time-activity curves of the heart, liver, and kidney from normal BALB/C nude mice administered with [^{64}Cu]CM-2 or [^{64}Cu]CM-3. (D) Time-activity curves of the bladder. Data represent the mean ± SD, n = 3.

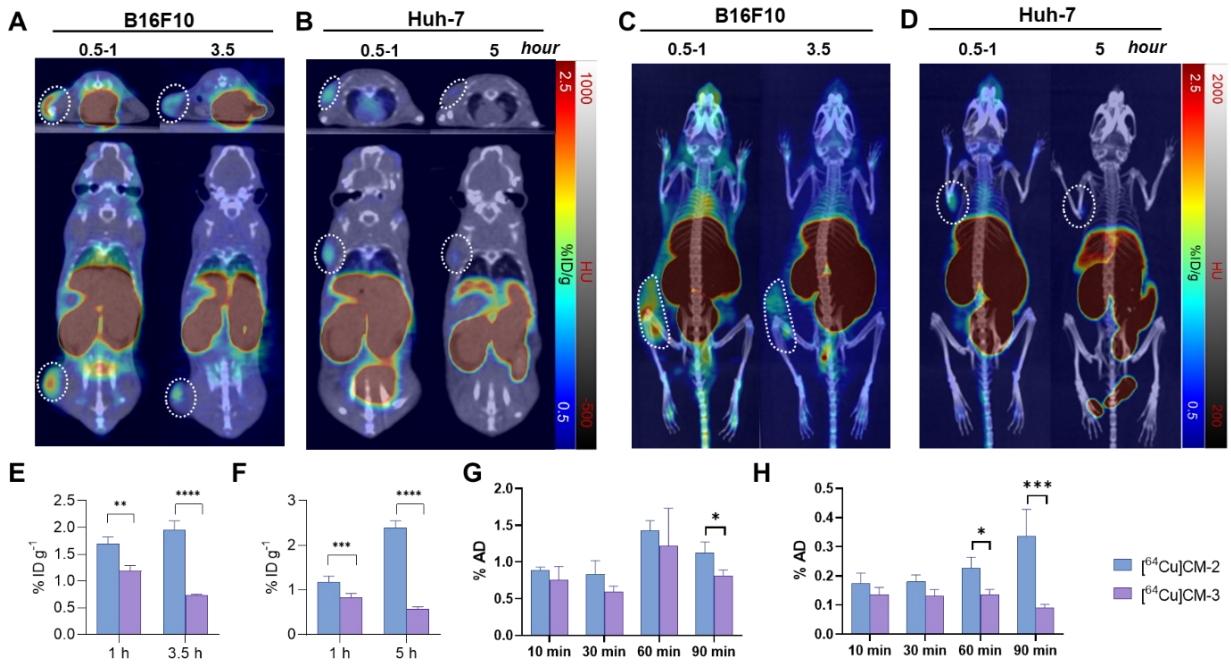

Figure S8. Series of co-registered PET-CT images of (A) B16F10-bearing C57BL/6J and (B) Huh-7-bearing BALB/C nude mice at different time points postinjection of [^{64}Cu]CM-3. The white dashed circles indicate the B16F10 tumors. Animals were injected with approximately 17 MBq (0.2 mL, approximately 0.5 nmol of CM-2) of the tracers per mouse via the tail vein. (C and D) The corresponding co-registered PCT-CT MIPs of A and B, respectively. Comparison of quantitative uptake of [^{64}Cu]CM-2 and [^{64}Cu]CM-3 in B16F10 (E) and Huh-7 (F) at different time point after injection. Comparison of cellular uptake of [^{64}Cu]CM-2 and [^{64}Cu]CM-3 in Huh-7 tumor cells (G) and B16F10 tumor cells (H) after co-incubation for different periods. Comparisons were performed using unpaired two-tailed Student's t-test. Data are presented as the mean ± SD, $n = 3$, ***$P < 0.001$, ****$P < 0.0001$.

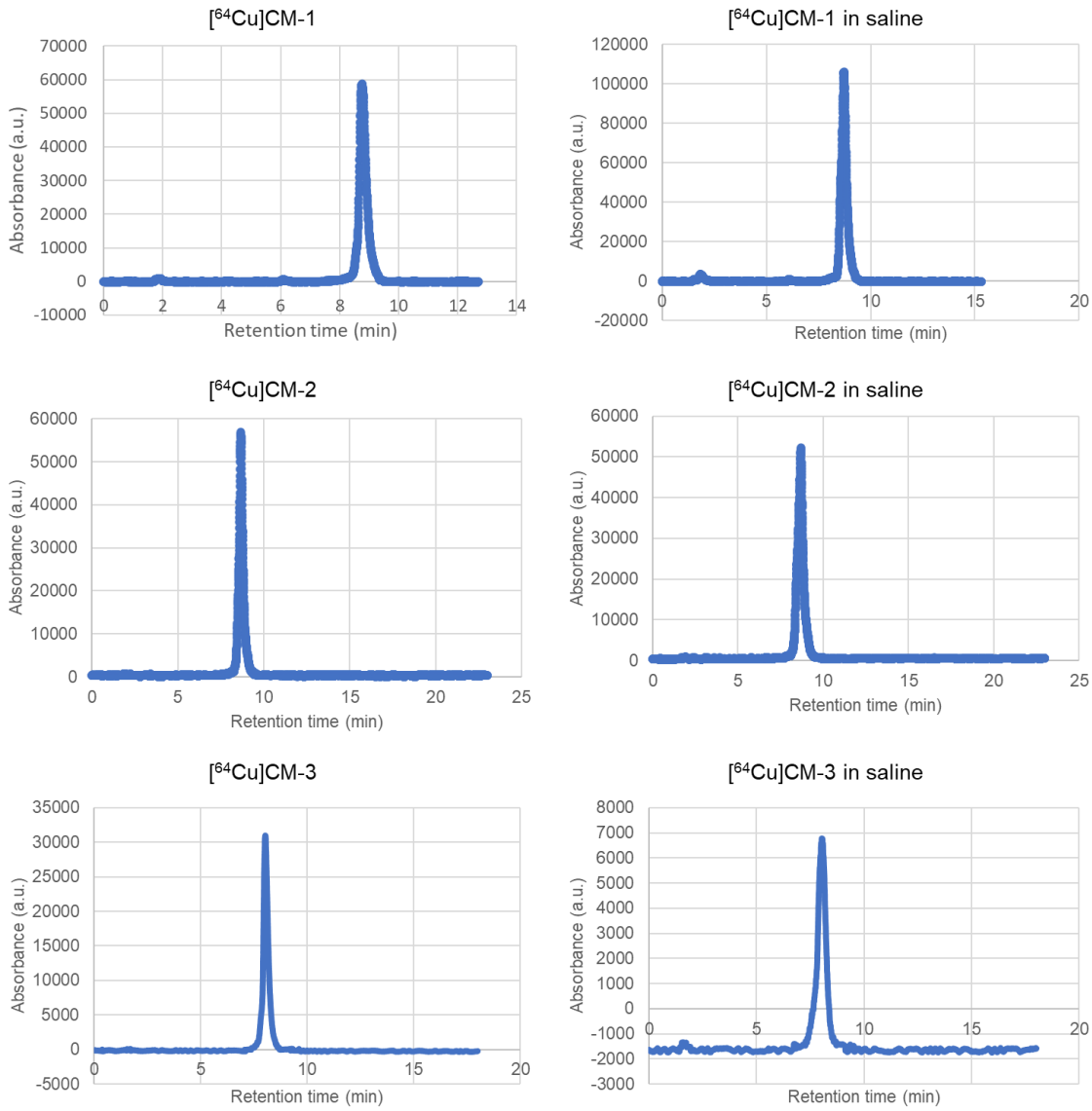

Figure S9. Radiosynthesis of [^{64}Cu]CM-1, [^{64}Cu]CM-2, and [^{64}Cu]CM-3, and their stability in saline

6. Supplementary HPLC curves and mass spectra

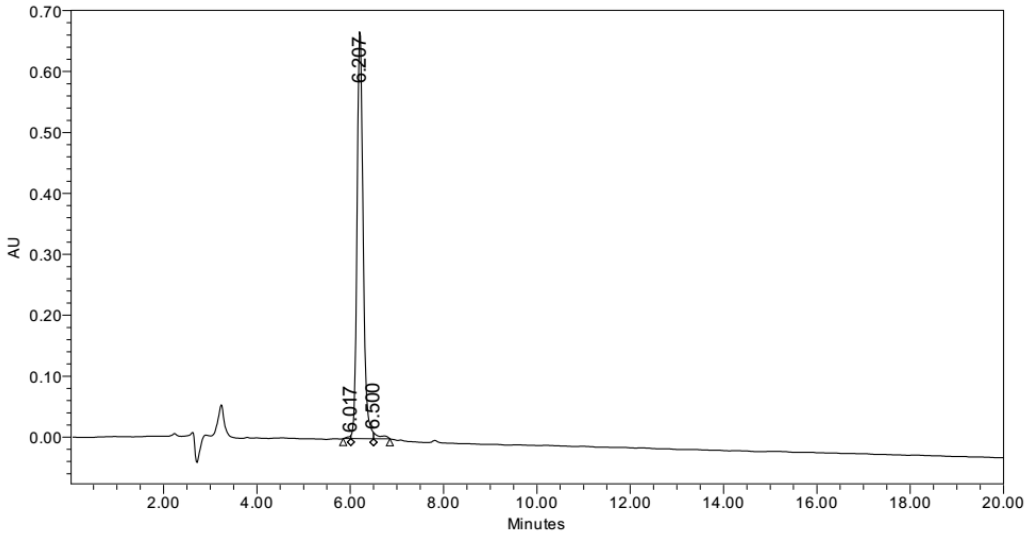

Figure S10. HPLC chromatogram of CM-1

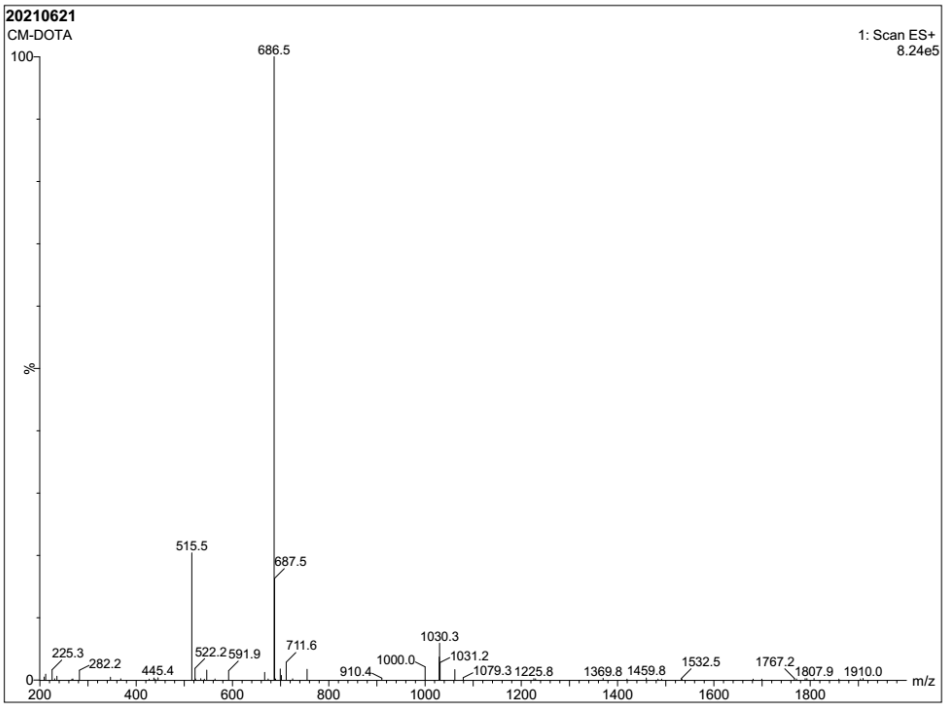

Figure S11. Mass spectrum of CM-1

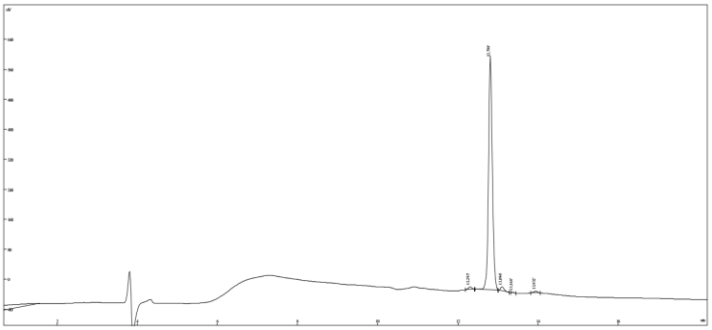

Figure S12. HPLC chromatogram of CM-2.

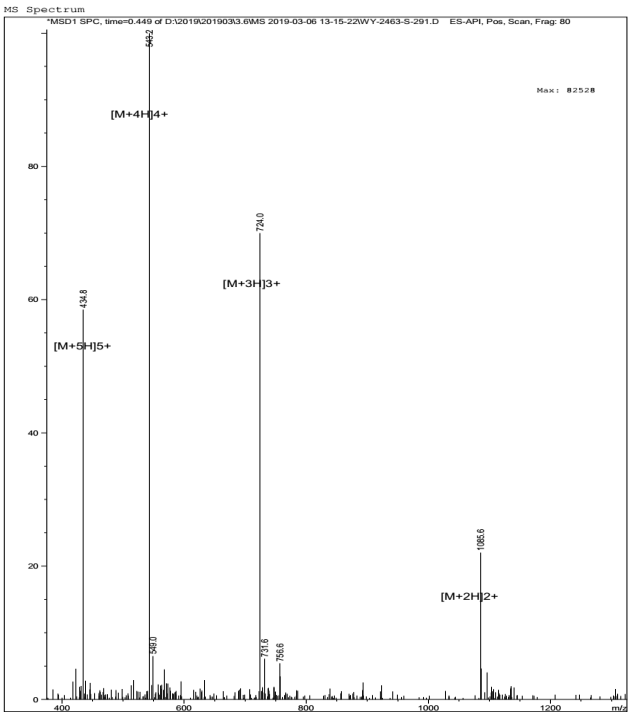

Figure S13. Mass spectrum of CM-2

(a) ESI full mass

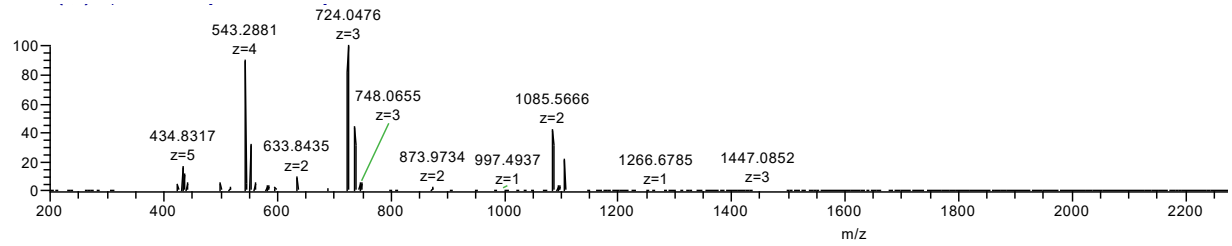

(b) Analysis of $[M/2+H]^{2+}$

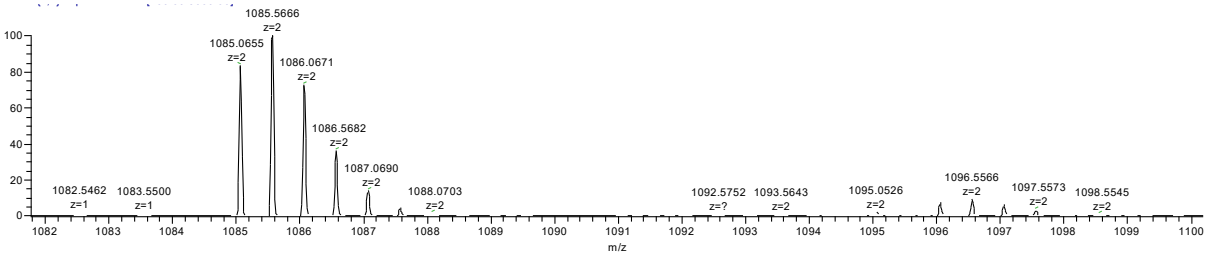

Figure S14. HRMS of CM-2.

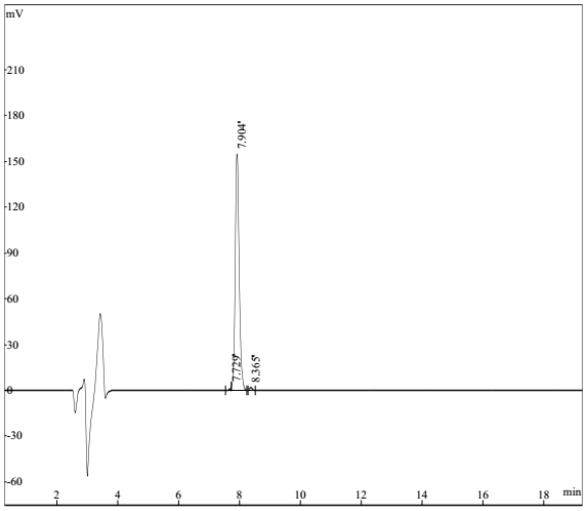

Figure S15. HPLC chromatogram of CM-3

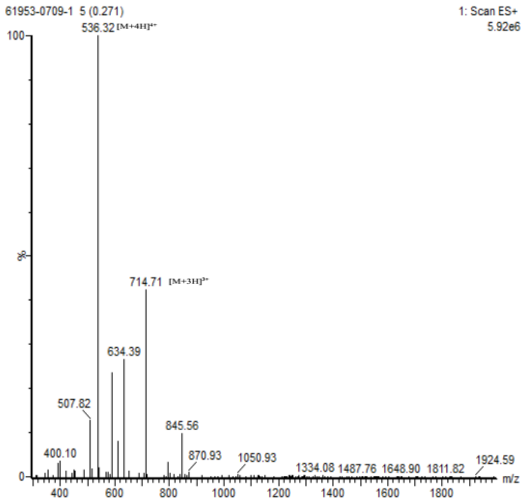

Figure S16. Mass spectrum of CM-3

(a) ESI Full mass

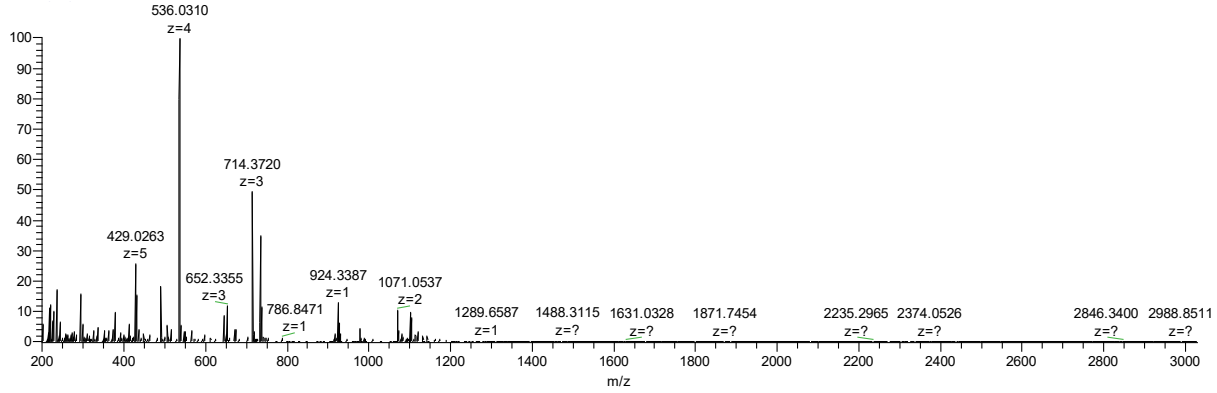

(b) Analysis of $[M/2+H]^{2+}$

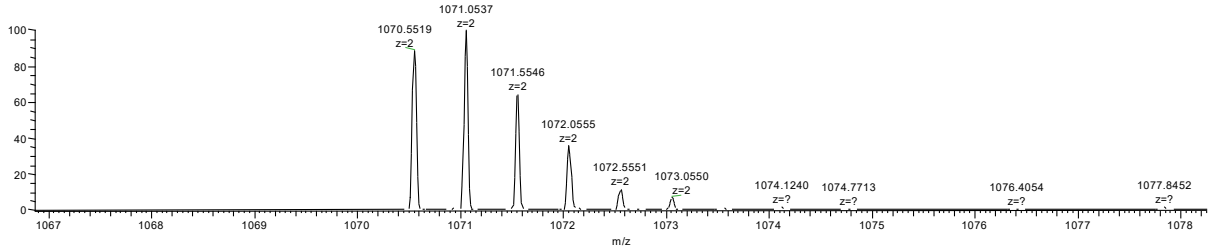

Figure S17. HRMS of CM-3.

Reference:

1. Gaedicke, S.; Braun, F.; Prasad, S.; Machein, M.; Firat, E.; Hettich, M.; Gudihal, R.; Zhu, X.; Klingner, K.; Schüler, J.; Herold-Mende, C. C.; Grosu, A.-L.; Behe, M.; Weber, W.; Mäcke, H.; Niedermann, G., Noninvasive positron emission tomography and fluorescence imaging of CD133⁺ tumor stem cells. *Proc. Natl. Acad. Sci. U. S. A.* **2014,** *111* (6), E692-E701.
2. Lang, J.; Lan, X.; Liu, Y.; Jin, X.; Wu, T.; Sun, X.; Wen, Q.; An, R., Targeting cancer stem cells with an 131I-labeled anti-AC133 monoclonal antibody in human colorectal cancer xenografts. *Nucl. Med. Biol.* **2015,** *42* (5), 505-512.
3. Glumac, P. M.; Gallant, J. P.; Shapovalova, M.; Li, Y.; Murugan, P.; Gupta, S.; Coleman, I. M.; Nelson, P. S.; Dehm, S. M.; LeBeau, A. M., Exploitation of CD133 for the Targeted Imaging of Lethal Prostate Cancer. *Clin. Cancer Res.* **2020,** *26* (5), 1054-1064.
4. She, X.; Qin, S.; Jing, B.; Jin, X.; Sun, X.; Lan, X.; An, R., Radiotheranostic Targeting Cancer Stem Cells in Human Colorectal Cancer Xenografts. *Mol. Imaging Biol.* **2020,** *22* (4), 1043-1053.
5. Wyszatko, K.; Valliant, J.; Sadeghi, S.; Singh, S., PET imaging cancer stem cells using a novel zirconium-89 labelled fully human anti-CD133 antibody. *J. Nucl. Med.* **2021,** *62* (supplement 1), 154-154.
6. Liu, Y.; Yao, X.; Wang, C.; Wang, M.; Wang, Y.; Ye, M.; Liu, Y., Peptide-based 68Ga-PET radiotracer for imaging CD133 expression in colorectal cancer. *Nucl. Med. Commun.* **2021**.